

# A “slingshot” laser-driven acceleration mechanism of plasma electrons

Gaetano Fiore<sup>1,3</sup>, Sergio De Nicola<sup>2,3</sup>

<sup>1</sup> Dip. di Matematica e Applicazioni, Università di Napoli “Federico II”,  
Complesso Universitario Monte Sant’Angelo, Via Cintia, 80126 Napoli, Italy

<sup>2</sup> SPIN-CNR, Complesso MSA, Via Cintia, 80126 Napoli, Italy

<sup>3</sup> INFN, Sez. di Napoli, Complesso MSA, Via Cintia, 80126 Napoli, Italy

We briefly report on the recently proposed [1, 2] electron acceleration mechanism named “slingshot effect”: under suitable conditions the impact of an ultra-short and ultra-intense laser pulse against the surface of a low-density plasma is expected to cause the expulsion of a bunch of superficial electrons with high energy in the direction opposite to that of the pulse propagation; this is due to the interplay of the huge ponderomotive force, huge longitudinal field arising from charge separation, and the finite size of the laser spot.

**Keywords:** Laser-plasma interactions, electron acceleration, magnetohydrodynamics

## I. INTRODUCTION

Today ultra-intense laser-plasma interactions allow extremely compact acceleration mechanisms of charged particles to relativistic regimes, with numerous and extremely important potential applications in nuclear medicine (cancer therapy, diagnostics), research (particle physics, inertial nuclear fusion, optics, materials science, structural biology,...), food sterilization, transmutation of nuclear wastes, etc. A prominent mechanism for electrons is the *Wake-Field Acceleration* (WFA) [3]: electrons are accelerated “surfing” a plasma wake wave driven by a short laser or charged particle beam within a low-density plasma sample (or matter to be locally completely ionized into a plasma by the beam, more precisely a supersonic gas jet), and are expelled just after the exit of the beam out of the plasma, behind and *in the same direction as the beam* (forward expulsion). WFA has proved to be particularly effective since 2004 in the so-called *bubble* (or *blowout*) regime; it can produce electron bunches of very good collimation, small energy spread and energies of up to hundreds of MeVs [4–6] or more recently even GeVs [7, 8].

In Ref. [1, 2] it has been claimed that the impact of a very short and intense laser pulse in the form of a pancake normally onto the surface of a low-density plasma may induce also the acceleration and expulsion of electrons *backwards* (*slingshot effect*), see fig. 1. A bunch of plasma electrons (in a thin layer just beyond the vacuum-plasma interface) first are displaced forward with respect to the ions by the positive ponderomotive force  $F_p \equiv \langle -e(\frac{\mathbf{v}}{c} \times \mathbf{B})^z \rangle$  generated by the pulse (here  $\langle \rangle$  is the average over a period of the laser carrier wave,  $\mathbf{E}, \mathbf{B}$  are the electric and magnetic fields,  $\mathbf{v}$  is the electron velocity, and  $\hat{\mathbf{z}}$  is the direction of propagation of the laser pulse; recall that  $F_p$  is positive, negative when the

modulating amplitude  $\epsilon_s$  of the pulse respectively increases, decreases), then are pulled back by the electric force  $-eE^z$  due to this charge displacement. If the electron density  $\tilde{n}_0$  is tuned in the range where the plasma oscillation period  $T_H$  is about twice the pulse duration  $\tau$ , then these electrons invert their motion when they are reached by the maximum of  $\epsilon_s$ , so that the negative part of  $F_p$  adds to  $-eE^z$  in accelerating them backwards; equivalently, the total work  $W \equiv \int_0^\tau dt F_p v^z$  done by the ponderomotive force is maximal[? ]. Their expulsion energy (out of the bulk) will be enough to escape to  $z \rightarrow -\infty$  if the laser spot radius  $R$  is suitably tuned.

The very short pulse duration  $\tau$  and expulsion time  $t_e$ , as well as huge nonlinearities, make approximation schemes based on Fourier analysis and related methods inconvenient. But recourse to full kinetic theory is not necessary: we show [2, 9] that in the relevant space-time region a MagnetoHydro-Dynamic (MHD) description of the impact is self-consistent, simple and predictive. The set-up is as follows. We describe the plasma as consisting of a static background of ions and a fully relativistic, collisionless fluid of electrons, with the system “plasma + electromagnetic field” fulfilling the Lorentz-Maxwell and the continuity Partial Differential Equations (PDE). For brevity, below we refer to the electrons’ fluid element initially located at  $\mathbf{X} \equiv (X, Y, Z)$  as to the “ $\mathbf{X}$  electrons”, and to the fluid elements with arbitrary  $X, Y$  and specified  $Z$  as the “ $Z$  electrons”. We denote: as  $\mathbf{x}_e(t, \mathbf{X})$  the position at time  $t$  of the  $\mathbf{X}$  electrons, and for each fixed  $t$  as  $\mathbf{X}_e(t, \mathbf{x})$  the inverse of  $\mathbf{x}_e(t, \mathbf{X})$  [ $\mathbf{x} \equiv (x, y, z)$ ]; as  $c$  the velocity of light; as  $m$  and as  $n, \mathbf{v}, \mathbf{p}$  the electrons’ mass and Eulerian density, velocity, momentum.  $\beta \equiv \mathbf{v}/c$ ,  $\mathbf{u} \equiv \mathbf{p}/mc = \beta/\sqrt{1-\beta^2}$ ,  $\gamma \equiv 1/\sqrt{1-\beta^2} = \sqrt{1+\mathbf{u}^2}$  are dimensionless. We assume that the plasma is initially neutral, unmagnetized and at rest with electron (and proton) density  $\tilde{n}_0(z)$  depending only on  $z$  and equal to zero in the

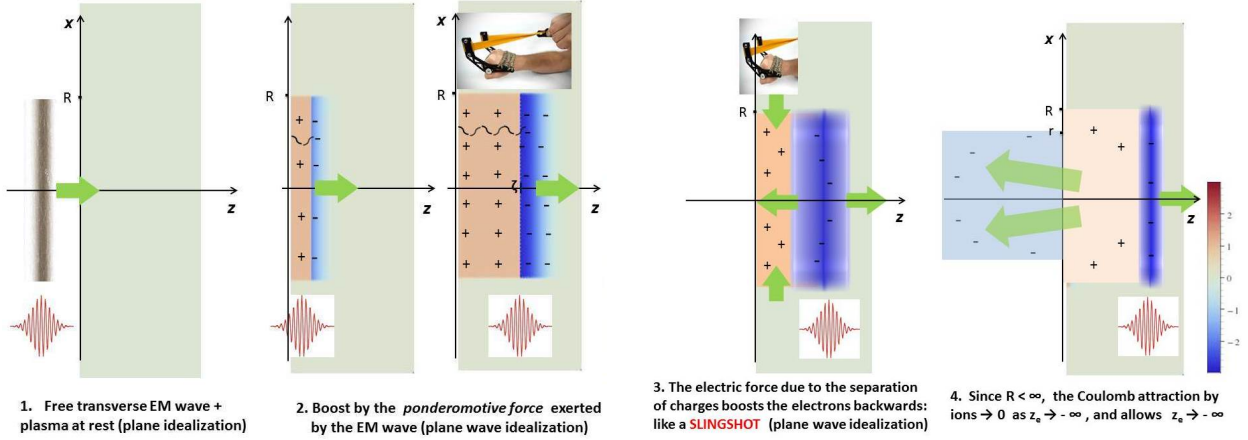


FIG. 1. Schematic stages of the slingshot effect

region  $z < 0$ . We schematize the laser pulse as a free transverse EM plane travelling-wave multiplied by a cylindrically symmetric “cutoff” function, e.g.

$$\mathbf{E}^\perp(t, \mathbf{x}) = \epsilon^\perp(ct - z) \theta(R - \rho), \quad \mathbf{B}^\perp = \hat{\mathbf{z}} \times \mathbf{E}^\perp \quad (1)$$

where  $\rho \equiv \sqrt{x^2 + y^2} \leq R$ ,  $\theta$  is the Heaviside step function, and the ‘pump’ function  $\epsilon^\perp(\xi)$  vanishes outside some finite interval  $0 < \xi < l$ . Then, to simplify the problem,

1. We first study the  $R = \infty$  (i.e. *plane-symmetric*) version, carefully choosing unknowns and independent variables (section II.1). For sufficiently small densities and short times we can reduce the PDE’s to a collection of decoupled *systems of two first order nonlinear ODE in Hamiltonian form*, which we solve numerically.

2. We determine (section II.2):  $R < \infty$ ,  $r > 0$  so that the plane version gives small errors for the surface electrons with  $\rho \leq r \leq R$ ; the corresponding final energy, spectrum, etc. of the expelled electrons. For definiteness, we consider the  $\tilde{n}_0(z)$  of fig. 2.

We specialize our predictions to virtual experiments at the FLAME facility (LNF, Frascati). We invite for simulations (PIC, etc.) and experiments testing them.

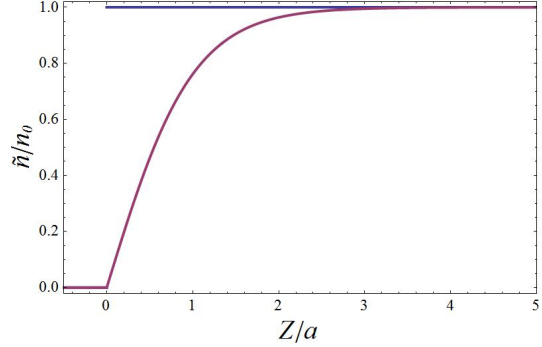


FIG. 2. The normalized  $\tilde{n}_0$  adopted here: step-shaped (blue) and continuous  $\tilde{n}_0(Z) = n_0 \theta(Z) \tanh(Z/a)$ ,  $a = 20\mu\text{m}$  (purple); they respectively model the initial electron densities at the vacuum interfaces of an aerogel and of a gas jet (just outside the nozzle).

## II. THE MODEL

### II.1. Plane wave idealization

Our plane wave Ansatz reads:  $A^\mu, \mathbf{u}, n - \tilde{n}_0(z)$  depend only on  $z, t$  and vanish if  $ct \leq z$ ;  $\Delta \mathbf{x}_e \equiv \mathbf{x}_e - \mathbf{X}$  depends only on  $Z, t$  and vanishes if  $ct \leq Z$ . Then:  $\mathbf{B} = \mathbf{B}^\perp = \hat{\mathbf{z}} \partial_z \wedge \mathbf{A}^\perp$ ,  $c\mathbf{E}^\perp = -\partial_t \mathbf{A}^\perp$ ; the transverse component of the Lorentz equation implies  $\mathbf{u}^\perp = e\mathbf{A}^\perp/mc^2$ ; due to charge separation  $E^z \neq 0$ : by the Maxwell equations it is related to the longitudinal motion through

$$E^z(t, z) = 4\pi e \left\{ \tilde{N}(z) - \tilde{N}[Z_e(t, z)] \right\}, \quad \tilde{N}(Z) \equiv \int_0^Z d\eta \tilde{n}_0(\eta), \quad (2)$$

what yields a conservative force on the electrons. For sufficiently small densities and short times the

laser pulse is not significantly affected by the interaction with the plasma (the validity of this approximation is checked a posteriori [2]), and we can identify  $\mathbf{A}^\perp(t, z) = \boldsymbol{\alpha}(\xi)$ ,  $\xi \equiv ct - z$ , where  $\boldsymbol{\alpha}$  is the transverse vector potential of the “pump” free laser pulse. Hence also  $\mathbf{u}^\perp(t, z) = e\boldsymbol{\alpha}(\xi)/mc^2$  is explicitly determined. For each fixed  $Z$ , the unknown  $z_e(t, Z)$  appears in place of  $z$  in the equations of motion of the  $Z$ -electrons. But, as no particle can reach the speed of light, the map  $t \mapsto \xi \equiv ct - z_e(t, Z)$  is strictly increasing, and we can use [2, 9]  $(\xi, Z)$  instead of  $(t, Z)$  as independent variables. It is also convenient to use the “electron  $s$ -factor”  $s \equiv \gamma - u^z$  instead of  $u^z$  as an unknown, because it is *insensitive* to rapid oscillations of  $\boldsymbol{\alpha}$ , and  $\gamma, \mathbf{u}, \beta$  are *rational* functions of  $\mathbf{u}^\perp$ ,  $s$ :

$$\gamma = \frac{1 + \mathbf{u}^{\perp 2} + s^2}{2s}, \quad u^z = \frac{1 + \mathbf{u}^{\perp 2} - s^2}{2s}, \quad \boldsymbol{\beta} = \frac{\mathbf{u}}{\gamma}. \quad (3)$$

Then the remaining PDE to be solved are reduced to the following collection of systems (parametrized by  $Z$ ) of first order ODE’s in the unknowns  $\Delta(\xi, Z), s(\xi, Z)$ :

$$\begin{aligned} \Delta' &= \frac{1+v}{2s^2} - \frac{1}{2}, & s' &= \frac{4\pi e^2}{mc^2} \left\{ \tilde{N}[\Delta + Z] - \tilde{N}(Z) \right\} \\ \Delta(0, Z) &= 0, & s(0, Z) &= 1. \end{aligned} \quad (5)$$

Here  $v(\xi) \equiv [e\boldsymbol{\alpha}(\xi)/mc^2]^2$ ,  $\Delta \equiv z_e - Z$ ,  $f' = \partial f / \partial \xi$ . Eq.s (4) can be written also in the form [9] of *Hamilton equations*  $q' = \partial H / \partial p$ ,  $p' = -\partial H / \partial q$  in 1 degree of freedom:  $\xi, -\Delta, s$  play the role of  $t, q, p$ . Solving (4-5) numerically all unknowns are determined. For  $z > 0$   $\mathbf{u}(t, z), n(t, z), \dots$  evolve as forward travelling waves.

In particular, if  $\tilde{n}_0(Z) = n_0\theta(Z)$  then (2) implies that the longitudinal electric force acting on the  $Z$ -electrons is

$$\tilde{F}_e^z(t, Z) = \begin{cases} -4\pi n_0 e^2 \Delta z_e = \text{elastic force} & \text{if } z_e > 0, \\ 4\pi n_0 e^2 Z = \text{constant force} & \text{if } z_e \leq 0; \end{cases} \quad (6)$$

hence as long as  $z_e \geq 0$  each  $Z$ -layer of electrons is an independent copy of the *same* relativistic harmonic oscillator, (4-5) are  $Z$ -independent and reduce to a *single* system of two first order ODE’s

$$\Delta' = \frac{1+v}{2s^2} - \frac{1}{2}, \quad s' = M\Delta, \quad (7)$$

$$\Delta(0) = 0, \quad s(0) = 1, \quad (8)$$

( $M \equiv 4\pi n_0 e^2 / mc^2$ ).  $n_0 \rightarrow 0$  implies  $s \equiv 1$ , and the equations are solved in closed form [10, 11]. In fig. 3 we plot a typical pump and the corresponding solution of (7-8).

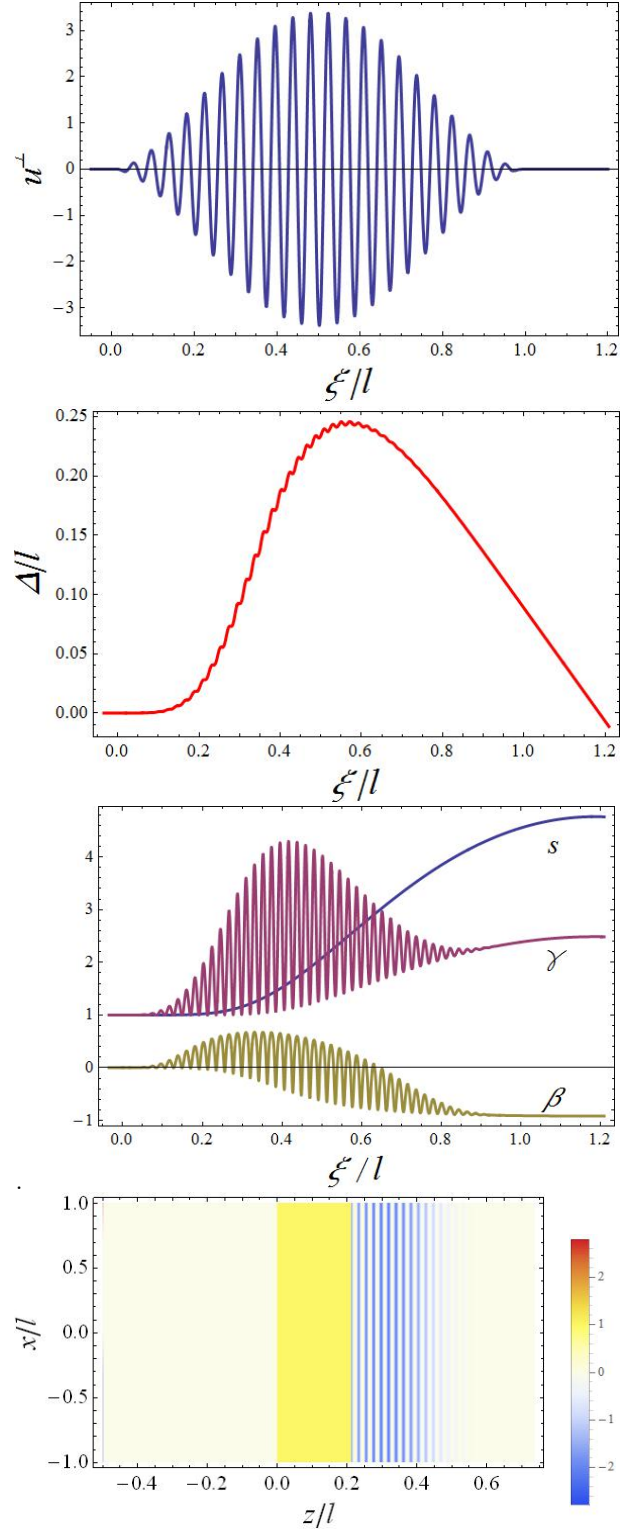


FIG. 3. Typical normalized pump amplitude  $\mathbf{u}^\perp = e\boldsymbol{\alpha}/mc^2$  vanishing outside  $0 < \xi < l$  (up), corresponding solution of (7-8) for  $Ml^2 = 26$  (center) and normalized charge density plot after 40 fs (down).

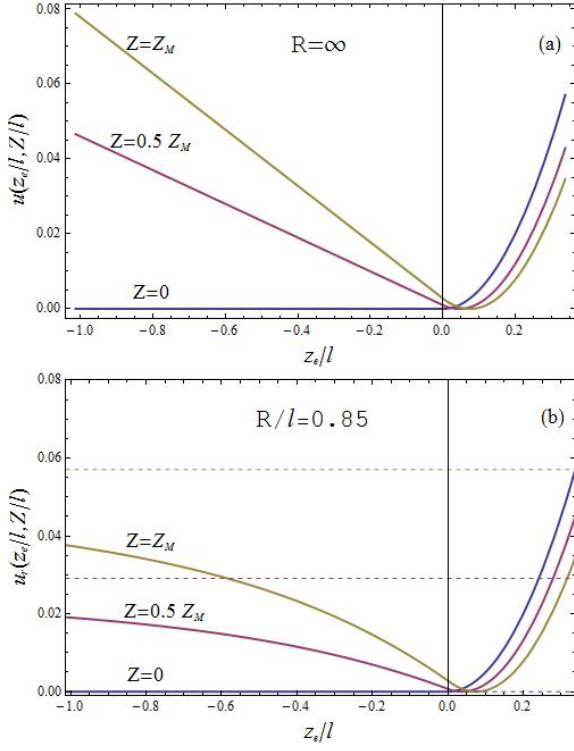


FIG. 4. Rescaled longitudinal electric potential energies  $u \equiv U/4\pi n_0 e^2 l^2$ ,  $u_r \equiv U_R/4\pi n_0 e^2 l^2$  in the case of step-shaped density  $\tilde{n}_0(Z) = n_0 \theta(Z)$  and (a) idealized plane wave or (b) for  $R/l = 0.85$ , vs. the dimensionless ratio  $z_e/l$  for  $Z=0$ ,  $Z=0.5Z_M$ ,  $Z=Z_M$ ; the horizontal dashed lines are the left asymptotes of  $u_r$  for the same values of  $Z$ .

## II.2. Finite $R$ corrections and experimental predictions

The results of the previous section can be applied to the small  $Z$  Forward Boosted Electrons (FBE) in the region  $\rho \lesssim R$ ; this leads to a cylinder  $C_R$  of the same radius completely deprived of electrons, with maximum height  $\zeta$  at the time  $\bar{t}$  of maximal penetration  $\zeta$  of the FBE. The displaced charges modify  $\mathbf{E}$ . By causality, for  $\mathbf{x}$  near the  $\bar{z}$  axis  $\mathbf{E}(t, \mathbf{x})$  is the same as in the plane wave case for  $t \lesssim \bar{t} + R/c$  (the “information about the finite  $R$ ” contained in the retarded fields takes a time  $R/c$  to go from  $\rho = R$  to  $\rho = 0$ ), and smaller afterwards. We tune  $R$  to fulfill

$$\frac{[t_e - \bar{t}]c}{R} \sim 1, \quad r \equiv R - \frac{\zeta(t_e - l/c)}{2(t_e - \bar{t})} \theta(ct_e - l) > 0 \quad (9)$$

( $t_e$  is the expulsion time of the FBE). Conditions (9) respectively ensure: that the motion of these FBE is close to the one in section II.1 until their expulsion, at least within an inner cylinder  $\rho \leq r \leq R$ ; that their expulsion takes place before lateral electrons, which

are initially located outside the surface of  $C_R$  and are attracted towards the  $\bar{z}$ -axis, obstruct them the way out [1, 2].

The expelled  $Z$  electrons are decelerated by the electric force  $\widetilde{F}_e^{zr} > 0$  generated by the net positive charge located at  $z > z_e(t, Z)$ , but  $\widetilde{F}_e^{zr} \propto 1/z_e^2$  as  $z_e \rightarrow -\infty$  since this charge is localized in  $C_R$ . Therefore we heuristically modify at  $z_e < 0$  the potential energies  $U(z_e, Z)$  associated to (2). If e.g.  $\tilde{n}_0(Z) = n_0 \theta(Z)$  then  $U(z_e, Z) = 2\pi n_0 e^2 [\theta(z_e) z_e^2 - 2z_e Z + Z^2]$  is modified for  $z_e < 0$  into

$$U_R(z_e, Z) = \pi n_0 e^2 \left[ (z_e - 2Z) \sqrt{(z_e - 2Z)^2 + R^2} - 4Z z_e - z_e \sqrt{z_e^2 + R^2} + 2Z^2 + 2Z \sqrt{4Z^2 + R^2} + R^2 \left( \sinh^{-1} \frac{2Z}{R} + \sinh^{-1} \frac{z_e - 2Z}{R} - \sinh^{-1} \frac{z_e}{R} \right) \right].$$

(see fig. 4). Solving the equations of motion we find that for sufficiently small  $Z$  ( $0 \leq Z \leq Z_M$ ) the map  $\mathbf{X} \mapsto \mathbf{x}_e(t, \mathbf{X})$  is one-to-one for all  $t$  (showing the *self-consistency* of this MHD treatment) and that  $z_e(t, Z) \xrightarrow{t \rightarrow \infty} -\infty$  (backward escape); some typical electron trajectories are shown in fig.’s 5, the animated versions are available at the hyperlink [people.na.infn.it/~gfiore/slingshot-videos](http://people.na.infn.it/~gfiore/slingshot-videos). The interplay of the ponderomotive, electric forces yield the longitudinal forward and backward drifts at the basis of the slingshot effect. On the contrary, transverse oscillations due to  $\mathbf{E}^\perp$  average to zero to yield vanishing final transverse drift and momentum, if - as usual - the pump (1) has a slow modulation  $\epsilon_s$  in the support  $0 < \xi < l$ :

$$\epsilon^\perp(\xi) = \hat{\mathbf{x}} \epsilon_s(\xi) \cos k\xi \quad \text{with } |\epsilon'_s| \ll |k\epsilon_s| \quad (10)$$

(here the pump is polarized e.g. in the  $x$ -direction) implies  $p^\perp(\xi) \simeq \epsilon_s(\xi) |\sin(k\xi)e/kc| = 0$  for  $\xi \geq l$ , and hence a good collimation of the expelled electrons. If the plasma is created by the impact on a supersonic gas jet (e.g. helium) of the pulse itself, then  $l < \infty$  is the length of the interval where the intensity is sufficient to ionize the gas.

On the contrary, deeper electrons ( $Z > Z_M$ ) are captured by the force  $\widetilde{F}_e^{zr}$  and circulate forth and back.

The EM energy  $\mathcal{E}$  carried by a pulse (1), (10) is

$$\mathcal{E} \simeq \frac{R^2}{8} \int_0^l d\xi \epsilon_s^2(\xi). \quad (11)$$

$\mathcal{E}$  is fixed and depends on the laser; reducing  $R$  (focalization) increases the intensity  $I$ , the electron penetration  $\zeta$  and the slingshot force, but we must not violate (9). In fact, (9) can be fulfilled with a rather small  $R$ .

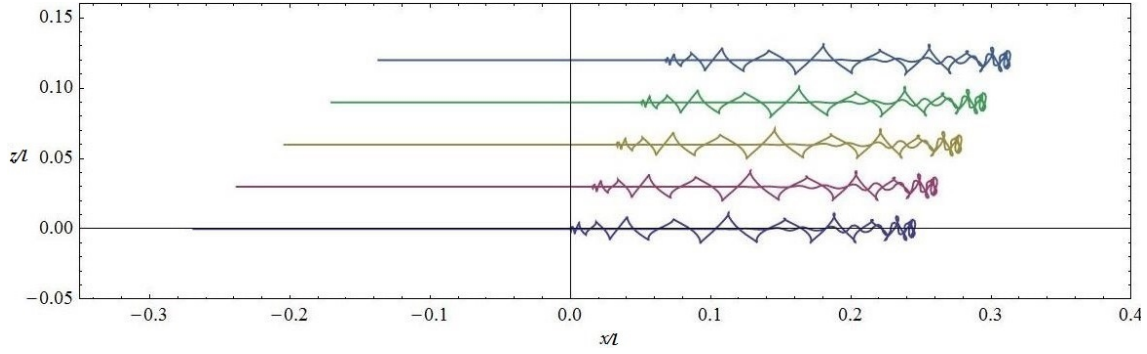


FIG. 5. Trajectories (after about 150 fs) of electrons initially located at different longitudinal positions:  $Z/Z_M = 0, 0.25, 0.5, 0.75, 1$ , from bottom up. The conditions are the same as in fig. 3.

We adopt a modulating amplitude of gaussian form

$$\epsilon_s^g(\xi) = b_g \exp[-(\xi - l/2)^2 / 2\sigma] \theta(\xi) \theta(l - \xi); \quad (12)$$

the parameters  $b_g, \sigma, l, \dots$  are determined by  $\mathcal{E}, R$  and the full width at half maximum  $l'$  of the pulse. We report in table I and fig. 6 sample results of extensive numerical simulations performed using as inputs the parameters available [12] in virtual experiments at the FLAME facility of the INFN Laboratori Nazionali di Frascati:  $l' \simeq 7.5 \mu\text{m}$  (corresponding to a time  $\tau' = 25\text{fs}$ ), wavelength  $\lambda \simeq 0.8 \mu\text{m}$ ,  $\mathcal{E} = 5\text{J}$ ,  $R$  tunable in the range  $10^{-4} \div 1\text{cm}$ ; a supersonic helium jet or an aerogel (if  $\tilde{n}_0(Z) = n_0 \theta(Z)$  with

$n_0 \gtrsim 48 \times 10^{18} \text{cm}^{-3}$ ) as targets. The energy spectrum, or equivalently the distribution  $\nu(\gamma_f)$  of the expelled electrons as a function of their final relativistic factor, depends dramatically on  $\tilde{n}_0, R$ ; pleasantly, in the case  $\tilde{n}_0(Z) = n_0 \theta(Z) \tanh(Z/a)$  it is very peaked (almost monochromatic) around  $\gamma_M$ , the maximal  $\gamma_f$ .

Summarizing, this new laser-induced “slingshot” acceleration mechanism should yield well-collimated bunches of electrons of energies up to few tens MeV. It is easily tunable and testable with present equipments.

**Acknowledgments** We thank R. Fedele for stimulating discussions, Compagnia di San Paolo for support under grant *Star Program 2013*.

- 
- [1] G. Fiore, R. Fedele, U. de Angelis, *Phys. Plasmas* **21** (2014), 113105.
  - [2] G. Fiore, S. De Nicola, arXiv:1509.04656.
  - [3] T. Tajima, J.M. Dawson, *Phys. Rev. Lett.* **43** (1979), 267.
  - [4] S. P. D. Mangles, et al., *Nature* **431** (2004), 535-538.
  - [5] C. G. R. Geddes, et al., *Nature* **431** (2004), 538-541.
  - [6] J. Faure, et al., *Nature* **431** (2004), 541-544.
  - [7] X. Wang, et al., *Nature Communications* **4** (2013), Article nr: 1988.
  - [8] W. P. Leemans, et al., *Phys. Rev. Lett.* **113** (2014), 245002.
  - [9] G. Fiore, *Travelling waves and a fruitful ‘time’ reparametrization in relativistic electrodynamics; A plane-wave model of the impact of short laser pulses on diluted plasmas*, in preparation.
  - [10] G. Fiore, *J. Phys. A: Math. Theor.* **47** (2014), 225501.
  - [11] G. Fiore, *Acta Appl. Math.* **132** (2014), 261-271.
  - [12] L.A. Gizzi, et al., *Appl. Sci.*, **3** (2013), 559-580.

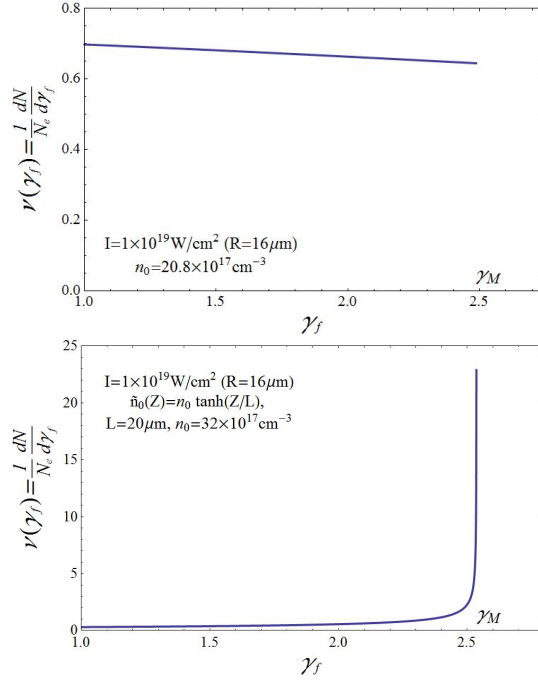


FIG. 6. Spectra of the expelled electrons for mean pulse intensity  $I=10^{19}$  W/cm<sup>2</sup> and step-shaped (up) or continuous (down)  $\tilde{n}_0$ .

pulse energy $\mathcal{E} \simeq 5$ J, wavelength $\lambda \simeq .8\mu\text{m}$ , duration $\tau' = 25$ fs							
type of target	h	h	h	h	h	a	a
pulse spot radius $R$ ( $\mu\text{m}$ )	16	8	4	2	2	2	1
mean intensity $I$ ( $10^{19}$ W/cm <sup>2</sup> )	1	4	16	64	64	64	255
initial density $n_0$ ( $10^{19}$ cm <sup>-3</sup> )	0.8	2	13	80	20	12	40
max. relativistic factor $\gamma_M$	2.6	6	8.5	14	21	12	23
max. expulsion energy (MeV)	1.3	3	4	7	11	6.4	12

TABLE I. Sample inputs and corresponding outputs if the target is: a supersonic helium jet (h) or an aerogel (a) with initial density profiles as in fig. 2. The expelled charge is in all cases a few  $10^{-10}$ C